Parallel confocal detection of single molecules in real time

Paul M. Lundquist, Cheng F. Zhong, Peiqian Zhao, Austin B. Tomaney, Paul S. Peluso, John Dixon,
Brad Bettman, Yves Lacroix, Deborah P. Kwo, Etienne McCullough, Mark Maxham, Kevin Hester,
Paul McNitt, Donald M. Grey, Carlos Henriquez, Mathieu Foquet, Stephen W. Turner,* and
Denis Zaccarin

Pacific Biosciences Inc., 1505 Adams Drive, Menlo Park, California 94025, USA
*Corresponding author: publications@pacificbiosciences.com

The confocal detection principle is extended to a highly parallel optical system that continuously analyzes thousands of concurrent sample locations. This is achieved through the use of a holographic laser illumination multiplexer combined with a confocal pinhole array before a prism dispersive element used to provide spectroscopic information from each confocal volume. The system is demonstrated to detect and identify single fluorescent molecules from each of several thousand independent confocal volumes in real time.   © 2008 Optical Society of America

OCIS codes: 180.1790, 170.2520, 350.4238, 170.6280, 310.6628, 300.2530.

Confocal microscopy is a powerful tool for the study of optical phenomena in diffraction-limited observation volumes [1]. It has been applied to single-molecule fluorescence spectroscopy [2] and has enabled the observation of chemical activity of biological molecules under physiological conditions [3]. The rejection of out-of-focus light allowed by the confocal geometry is important for detecting individual fluorescent molecules. For applications that require spatial multiplexing, such as screening assays and imaging, scanning confocal microscopy has been applied to a grid of observation volumes by raster scanning the illumination and detection volumes [4] or the sample itself [5]. This approach allows the reconstruction of numerous spatial positions but is limited in frame rate and cannot provide continuous observation. A variety of optical techniques including spatial filtering and microlens arrays have been used to generate complex steady-state illumination patterns (a review is found in Chap. 13 of [1]). Programmable array microscopes have been used to provide adjustment of the illumination pattern generated in a microscope, allowing highly flexible scanning confocal systems [6]. Approaches using polarizing beam splitters have allowed simultaneous monitoring of two detection volumes to facilitate correlation and motion analysis [7]. Confocal systems with spectroscopic capabilities have been demonstrated for several detection volumes [8], but real-time confocal systems with large multiplex and single-molecule sensitivity have not been reported.

We present here a system that provides several thousand continuously monitored confocal observation volumes with single-molecule sensitivity and spectroscopic resolution. In this system (Fig. 1), a monochromatic laser beam is divided by a wavelength-specific holographic phase mask (HPM) [9] into several thousand sub-beams propagating in a uniform rectangular array of k vectors. A relay lens assembly converts these beams into the corresponding array of spots focused at a plane conjugate to the front focus of a microscope objective (Olympus

UPLAPO $60\times$, NA 0.90). Multiple wavelength excitation can be achieved by combining the different wavelength paths with dichroic filters (for example, Semrock Di01-T488/532/638-25$\times$36). All of the illumination light is transmitted through a common dichroic and brought to an array of diffraction-limited spots in the sample plane where it excites fluorescence in each observation volume whenever a fluorescent molecule is present. The emitted light is collected in epifluorescence mode and deflected 90° by the dichroic filter. The deflected light is imaged onto a congruent array of confocal pinholes and then reimaged through a prism assembly onto a detector array. In this configuration, extra space is allowed between rows of observation volumes so that the spectral content of the emitted fluorescence can be dispersed (see
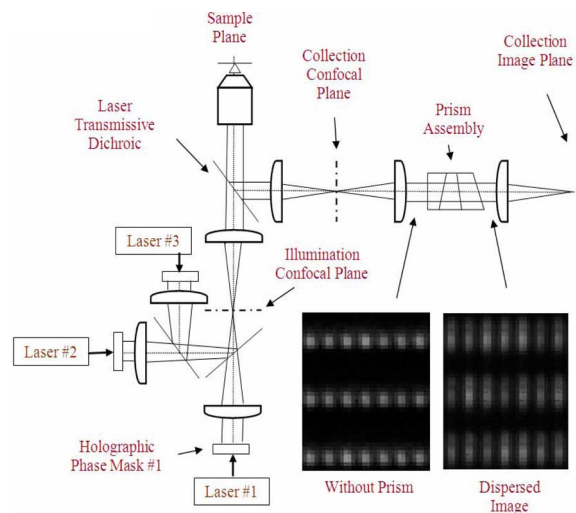

Fig. 1. (Color online) Schematic diagram of reversed confocal illumination and spectroscopy scheme. The images from multiple HPMs are superimposed at the illumination confocal plane. To exploit optimum dichroic filter design (narrow excitation bandwidths and high fluorescence throughput), the usual positions of the illumination and collection paths have been reversed. A pinhole array is placed at the confocal plane of the collection path to reject out-of-focus light.

Fig. 1 inset), allowing a single camera to collect both spatial and spectral information.

Holographic phase masks can be designed to divide a beam into an arbitrarily large number of spots. Other approaches such as microlens arrays have been applied to confocal systems to provide a targeted monochromatic illumination pattern [10], but HPMs allow greater flexibility in the spot arrangement and the spot profile. The HPM is very insensitive to lateral misalignment, provided the size (12 mm square in our case) is larger than the incident beam. An $M \times N$ array of phase pixels in the holographic mask's unit cell will result in a corresponding $M \times N$ array of output k vectors in which the beam centered around each k vector can have an independently assigned relative intensity. This freedom could be used to develop irregular patterns with different intensities for applications requiring diverse special-purpose observation volumes (see Chap. 4 of [9]). We have applied this freedom to create a rectangular array with uniform intensity (Fig. 2). The HPMs used in this system comprise periodic arrays of 64 gray-scale phase pixels (details vary somewhat for the different wavelength designs; in the 488 nm case the unit cell is 1098×1464 pixels, each 1 μm square). While this particular array configuration could be used to produce over 1.5×10^6 beams, more are possible with larger unit cells.

Confocal systems require a limiting aperture for critical detection [11]. This concept is extended to an array of 50 μm diameter pinholes congruent with the illumination spot array. The image of fluorescence light collected from a single confocal observation vol-

ume is shown in Fig. 3. Interference filters are commonly used for fluorescence color separation, but this approach is problematic in cases where a number of different spectra must be resolved or there is significant overlap between spectra. Continuous color separation can be provided by diffraction gratings, but poor efficiency ($\sim$80%) and lack of adjustability in the dispersion are disadvantageous. Here a prism assembly is chosen to provide continuous color separation and high transmission. Oversampling of the fluorescence spectra in wavelength improves the accuracy of classification in cases with overlapping emission. In our implementation, a three-wedge compound prism was optimized to provide linear dispersion as well as zero deviation angle at 550 nm. The prism provides an angular dispersion of 1.25 mrad between the wavelengths of 490 and 730 nm. With this choice, the system can be applied to a variety of fluorophore combinations. If resolution of highly overlapping emission spectra were a limitation, dispersion could be increased in the critical regions to improve spectral performance.

Confocal systems with single-molecule sensitivity have traditionally employed high-gain detectors, such as photomultiplier tubes (PMT) or avalanche photodiodes (APD). While these detectors are becoming available in multiplexed formats, megapixel-scale arrays are presently available only in CMOS and CCD technology. We employ an Andor iXon+ CCD camera with monolithically integrated electron-multiplication charge-coupled device (EMCCD) and frame-transfer capability. This enables continuous monitoring at frame rates of hundreds of hertz.

The technologies and approaches described above have been integrated into an instrument that can simultaneously perform single-molecule detection and spectroscopy on several thousand observation sites, providing the resolution and out-of-focus noise rejection that is available from a standard confocal microscopy scheme. An important application of multiplexed confocal microscope is the observation of fluorescence from arrayed optical confinement structures, such as nanocapillaries [12], silver-
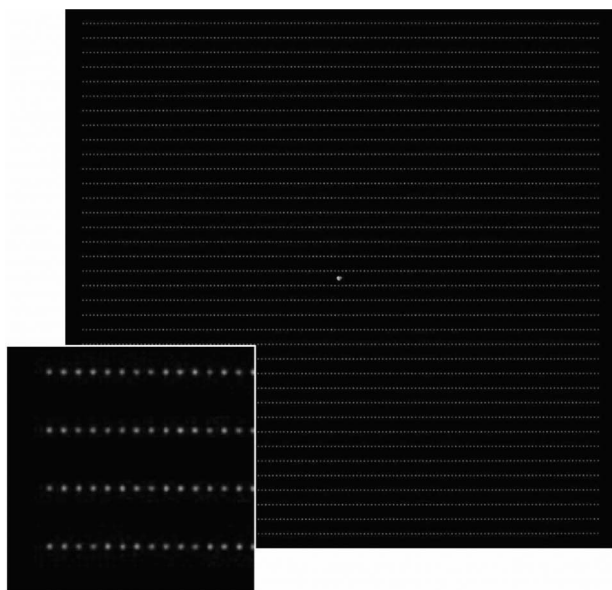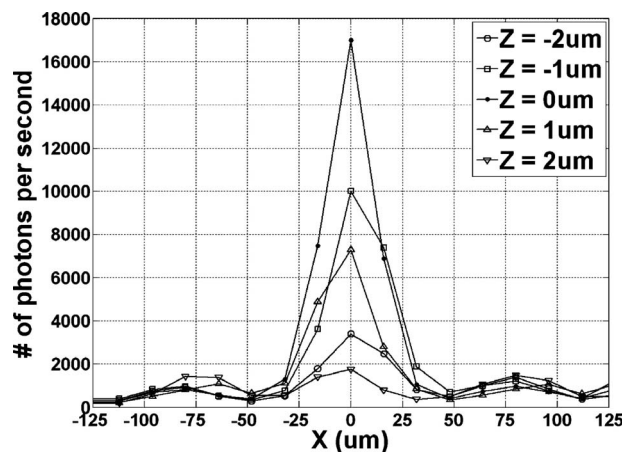

Fig. 2. Multiple-spot illumination pattern at the front focal plane of the microscope objective lens. This pattern was generated using 488 nm laser light divided into 5114 beams by a computer-generated HPM. The image was acquired using a thin film of fluorescent polymer spin coated on a glass substrate placed in the sample plane of the system with the prism removed. The inset is a magnified section from the corner of the optical field. Undiffracted laser light (0.2% of the total) appears near the center of the pattern. The overall variation in spot intensity is within ±15%.

Fig. 3. Point-spread function of Alexa-488 fluorescence light collected at the image plane for optimal focus as well as ±1 and 2 μm defocus. The 16 μm camera pixel size corresponds to 0.266 μm in the sample plane.

nanoparticle arrays [13], or zero-mode waveguides (ZMWs) [14]. To demonstrate our system, we selected an array of ZMWs because these structures enable fast real-time detection of molecular binding events that benefit from the continuous monitoring ability of our system. For the data presented here, we used transient binding of four different fluorescent molecular probes diffusing in solution: Alexa-488, Alexa-532, Alexa-568, and Alexa-647.

To excite the fluorophores, cw light from three lasers was used with wavelengths 488, 532, and 643 nm. The maximum power supplied by the lasers was 20, 20, and 30 mW, respectively, and the power levels were adjusted to provide 6.5 μW per spot at each wavelength. The spot size was adjusted to 0.80 μm FWHM in the image plane of the objective, which corresponds to a peak power density of 5.0 μW/μm^2. A grid of ZMWs (spaced 1.33×4.00 μm apart) was imaged through the optical system at an overall magnification of 60$\times$ and onto an EMCCD camera having 512×512 pixels. This corresponds to a maximum field position of 1.2° for which the objective provides field curvature and longitudinal chromatic aberration less than 100 nm with good image quality. Data were collected at a frame rate of 100 Hz (Fig. 4). Upon binding of a fluorophore inside the observation volume, there is an increase in the rate of fluorescence emission over the background level, ending upon release or bleaching of the fluorophore. In the system demonstrated here, these single-molecule fluorescence bursts provide 1000 photons or more at the detector. At this spacing, optical cross talk between neighboring observation volumes is quite low. To estimate the amount of cross talk we tabulated the integrated pulse amplitude of several hundred pulses observed from one observation volume and plotted these data against the integrated pulse amplitude over the same time period from an adjacent observation volume. Linear regression analysis for these data provides a cross talk value of 0.3%. For spectral analysis, light collected by the detector was summed over the duration of the burst allowing each individual fluorescent molecule to be spectrally evaluated and classified. The emitted light is linearly dispersed across 15 CCD pixels, which corresponds to 15 nm per pixel. The optical signal-to-noise ratio (SNR) varies over the four fluorescence channels used here. Peak intensities during a fluorescence burst are between 10 and 20 sigma above baseline and integrated burst intensities of 30 sigma and higher are observed. Unambiguous identification of the fluorescence source is achieved using automated classification of fluorescence sources by least-squares fitting to the four known spectra. The degree of spectral cross talk between different fluorophore types can be qualitatively seen from Fig. 4. The impact was estimated by a Monte Carlo simulation of optical noise, which indicated that under these conditions, misidentification rates with this method are much less than 1%. Larger multiplex values can be readily configured, but the SNR will be reduced as increasing laser power is applied to the system.

The approach to multiplexed confocal fluorescence microscopy demonstrated here can be applied to important problems in biotechnology. The capacity to identify multiple fluorescent species in real time with high fidelity over thousands of observation volumes is of particular interest for the application of single-molecule real-time DNA sequencing.
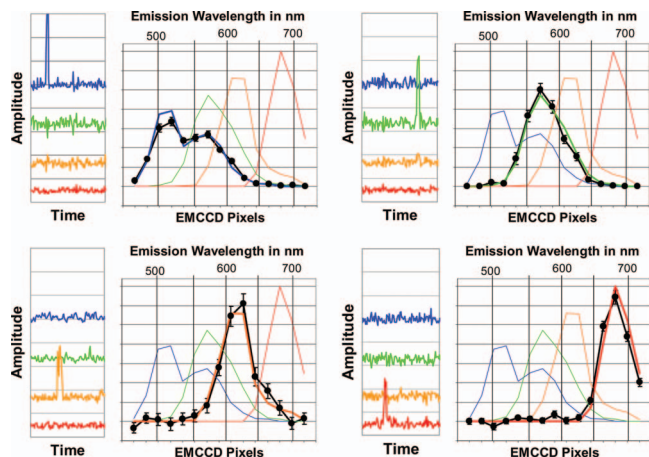

Fig. 4.   Example time traces (left) and spectra (right) collected from one observation volume at different times. Each of the four colors represents one spectral channel from a multicomponent analysis of the dispersed light collected from the observation volume. In the spectral plots, the solid colored curves represent reference spectra collected from each of the four fluoropohores in a calibration process. In each plot the black curve with error bars represents the photon flux integrated over the duration of the burst as a function of relative spectral position. The shown fluorescence bursts represent integrated burst SNR ratios between 20 and 35.

References

1. J. B. Pawley, *Handbook of Biological Confocal Microscopy*, 3rd ed. (Springer, 2006).
2. S. Weiss, Science **283**, 1676 (1999).
3. W. E. Moerner and L. Kandor, Anal. Chem. **61**, A1217 (1989).
4. G. Q. Xiao, T. R. Corle, and G. S. Kino, Appl. Phys. Lett. **53**, 716 (1988).
5. T. Wilson, J. N. Gannaway, and P. Johnson, J. Microsc. **118**, 390 (1980).
6. Q. S. Handley and T. J. Jovin, Appl. Spectrosc. **55**, 1115 (2001).
7. J. Jung and A. Van Orden, J. Am. Chem. Soc. **128**, 1240 (2006).
8. H.-S. Chon, G. Park, S.-B. Lee, S. Yoon, J. Kim, J.-H. Lee, and K. An, J. Opt. Soc. Am. A **24**, 60 (2007).
9. B. Kress, *Digital Diffractive Optics: an Introduction to Planar Diffractive Optics and Related Technology*, (Wiley, 2000).
10. M. Eisner, N. Lindlein, and J. Schwider, Opt. Lett. **23**, 748 (1998).
11. C. J. R. Sheppard and C. J. Cogswell, Scanning **13**, 240 (1991).
12. M. Foquet, J. Korlach, W. Zipfel, W. W. Webb, and H. G. Craighead, Anal. Chem. **74**, 1415 (2002).
13. T. D. Corrigan, S. Guo, R. J. Phaneuf, and H. Szmacinski, J. Fluoresc. **15**, 777 (2005).
14. M. Levene, J. Korlach, S. W. Turner, M. Foquet, H. G. Craighead, and W. W. Webb, Science **299**, 682 (2003).